RBAV Revista Brasileira de Aplicações de Vácuo
https://doi.org/10.17563/rbav.v45i1.1266
ORIGINAL PAPER

OPTICAL DETECTION OF A PRESSURE MICROSENSOR

Marcelo Bariatto Andrade Fontes[1,*], Eduardo Acedo Barbosa[2], Ruy Marcelo de Oliveira Pauletti[3], Francisco Tadeu Degasperi[4]

1. Faculdade de Tecnologia do Estado de São Paulo – Divisão de Microeletrônica – São Paulo (SP), Brazil.

2. Faculdade de Tecnologia do Estado de São Paulo – Divisão de Ensino Geral – São Paulo (SP), Brazil.

3. Universidade de São Paulo – Escola Politécnica – São Paulo (SP), Brazil.

4. Faculdade de Tecnologia do Estado de São Paulo – Divisão de Microeletrônica – São Paulo (SP), Brazil.

Corresponding author: bariatto@fatecsp.br

Section Editor: Mariana Fraga

Received: Nov. 6, 2025 **Approved:** Apr. 30, 2026

ABSTRACT

Microelectromechanical systems technology consists of manufacturing sensors and actuators on a micrometric scale, offering low response time, reproducibility, high sensitivity, and low manufacturing costs. Pressure microsensors have a wide range of applications in various areas, such as the automotive industry, production processes, medical equipment, and as an absolute pressure and vacuum sensor. The pressure microsensor developed is based on piezoresistors diffused on a silicon membrane, obtained by the anisotropic corrosion process. The standard response of the microsensor is electrical, obtained through a Wheatstone bridge circuit, in which the potential difference is a function of the resistance variation of the piezoresistors subjected to pressure. This work focused on the direct determination of the deflection of the membrane under pressure through optical measurements using a Michelson interferometer, thus obtaining a calibration curve (membrane deformation × pressure) providing a potential application as an absolute pressure and vacuum sensor. The experimental results were compared with theoretical and simulated values using the COMSOL Multiphysics simulator. The optical results indicated a linear relationship between membrane deformation and measured pressure, resulting in 3.61 μm/bar. Theoretical and simulated models suggest that the sensor's mounting is between free clamping and fully clamped.

KEYWORDS: Pressure Microsensor, Microelectromechanical Systems, Optical Interferometry, Vacuum-Pressure Metrology, Production Systems.

DETECÇÃO ÓPTICA DE UM MICROSENSOR DE PRESSÃO

RESUMO

A tecnologia de sistemas microeletromecânicos consiste na fabricação de sensores e atuadores na escala micrométrica, apresentando baixo tempo de resposta, reprodutibilidade, alta sensibilidade e baixo custo de fabricação. Os microssensores de pressão têm ampla gama de aplicações, em diversas áreas, tais como: indústria automotiva, processos de produção, equipamentos médicos e como sensor absoluto de pressão e vácuo. O microssensor de pressão desenvolvido é baseado em piezoresistores difundidos sobre uma membrana de silício, obtida pelo processo de corrosão anisotrópica. A resposta padrão do microssensor é elétrica, obtida por meio de um circuito em ponte de Wheatstone, no qual a diferença de potencial é função da variação de resistência dos piezoresistores submetidos à pressão. Este trabalho teve como foco a determinação direta da deflexão da membrana sob pressão, por intermédio de medidas ópticas, utilizando um interferômetro de Michelson, obtendo-se assim uma curva de calibração (deformação da membrana × pressão), possibilitando um sensor absoluto de pressão e vácuo como potencial aplicação. Os resultados experimentais foram comparados com valores teóricos e simulados pelo simulador COMSOL Multiphysics. Os resultados ópticos indicaram uma relação linear entre a deformação da membrana e a pressão medida, resultando em 3,61 μm/bar. Modelos teóricos e simulados sugerem que o engastamento do sensor se encontra entre o engastamento livre e o totalmente engastado.

PALAVRAS-CHAVE: Microssensor de Pressão, Sistemas Microeletromecânicos, Interferometria Óptica, Metrologia de Vácuo Pressão, Sistemas Produtivos.

INTRODUCTION

The technology used in the fabrication of microelectromechanical systems (MEMS) is multidisciplinary in nature, combining concepts from microelectronics, mechanical engineering, materials science, physics, and chemistry to produce integrated systems on a single chip, generating devices capable of performing sensing, control, and actuation functions, with advantages of large scale production, low manufacturing cost, high reproducibility, reliability, and low response time[1].

Developed since the 1980s, this technology has been evolving rapidly due to the wide range of possible applications, including vacuum technology and its metrology, and is considered one of the most promising technologies of the 21st century[2]. Pressure microsensors have a wide range of applications in various areas, ranging from the automotive industry to production processes and medical equipment[3].

There are several types of sensors that perform the mechanical transduction necessary for pressure measurement, based on the effects of piezoresistivity, piezoelectricity, variable capacitance, optics, and resonance. These pressure sensors are direct, meaning that pressure measurement does not depend on the type of gas[4]. Pressure measurement is based on the definition of pressure: the intensity of the normal force on the surface divided by the surface area. The definition depends exclusively on the transfer of linear momentum at the surface in which the molecules collide. Despite all the sophisticated technology available nowadays, there are few types of direct sensors available for use at pressures lower than atmospheric pressure. This proposed pressure sensor may be a viable and low-cost alternative for direct pressure measurement.

The developed microsensor is based on the use of four n-type silicon piezoresistors diffused on a p-type silicon membrane with a 5-mm side, obtained by the MEMS process, with a square dimension of 15 mm per side, 5 mm aluminum contacts, and piezoresistors with a line width of 250 μm, in which 12 microsensors were manufactured on a silicon wafer (100) with a diameter of 7.5 cm (Fig. 1)[5]. The standard electrical response of the microsensor (Vout), obtained by the Wheatstone bridge circuit, is given by Eq. 1:

$$V_{out} = \left(\frac{R3}{R3+R1} - \frac{R4}{R2+R4}\right).VCC \quad (1)$$

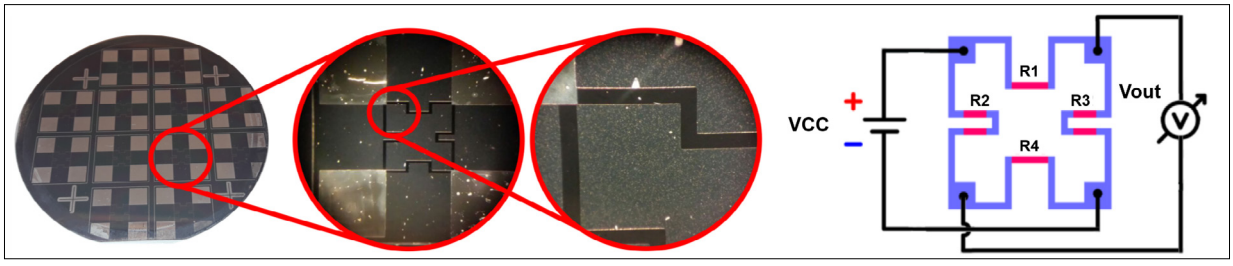

Figure 1: Silicon wafer containing manufactured microsensors and the Wheatstone bridge circuit used for their electrical characterization. Source: Sanches et al.[5].

A detection method explored in this project, different from the electrical one, refers to the direct determination of the membrane deflection through optical measurements, using a Michelson interferometer, schematically represented in Fig. 2. In the interferometer, a laser beam with a wavelength of λ is divided into two parts by partial reflection in the beam splitter DF (a semi-reflective mirror). These beams normally strike the flat mirrors E1 and E2 and are then reflected back to the splitter DF, in which they are recombined and undergo interference[6].

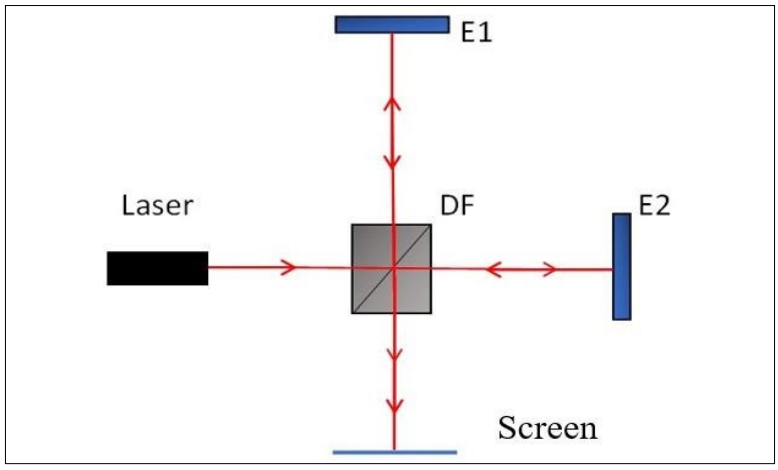

Figure 2: Schematic diagram of the Michelson interferometry measurement method.

Source: Elaborated by the authors.

If d1 and d2 are the lengths of arms 1 and 2, respectively, the difference between the paths of the two waves is 2d2–2d1, and any change in this difference will cause a modification in the interference pattern. For example, if mirror E2 is displaced by a distance equal to λ/2, the difference between the paths will vary by λ and the interference pattern will undergo a displacement of one fringe (each maximum will shift to the position of the neighboring maximum)[7,8].

In this project, a He-Ne laser (λ = 632.8 nm) was used, shining on the center of the pressure sensor membrane. It is then possible to measure displacements of λ/2 or 316.4 nm in the deflection of the membrane. Thus, by moving the fringes associated with the deflection of the sensor membrane due to the application of pressure, the displacement × pressure calibration is obtained. Another laser with a wavelength of 655 nm was also used for comparison. The experimental results were compared with theoretical and simulated values using the COMSOL Multiphysics simulator[9].

METHODS

In optical detection, a rigid support is essential to provide the necessary stability, since in this case only the deflection of the sensor membrane should alter the optical path. Thus, a metal flange with a central hole in the rear region was used, a polyflow tube was connected to a vacuum pump, and the sensor was fixed with silicone grease on the rear face (Fig. 3).

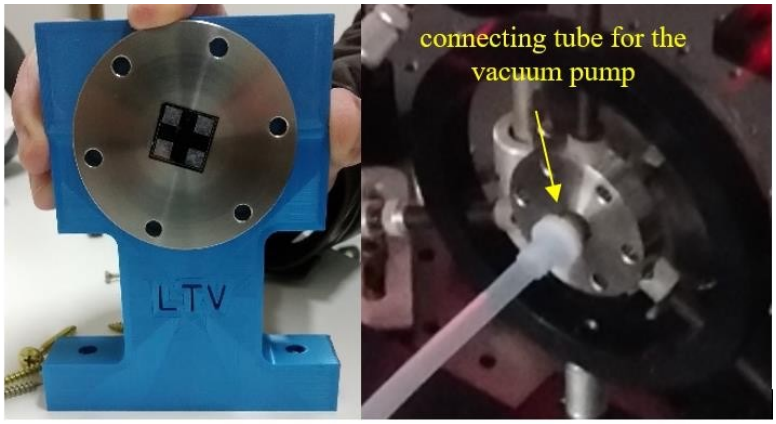

Figure 3: Metal base for fixing the pressure sensor for optical analysis.

Source: Elaborated by the authors.

The interferometer was assembled at Applied Optics Laboratory of FATEC-SP, on a table with pneumatic shock absorbers, in addition to techniques developed at the Vacuum Technology Laboratory of FATEC-SP. The measuring apparatus, shown schematically in Fig. 4, consists of a metal base on which the laser light is reflected by the central region of the sensor—acting as a high-reflecting mirror— in which the membrane is located, as well as a beam-splitter cube BS, and a second mirror M, with the interference pattern formed with the help of lens L for magnified viewing onto an opaque screen (used in this work) or onto a CCD camera for automatic analysis of the interference fringes. Figure 5 shows the details of the experimental assembly and of the fringe pattern projection. All measurements occurred at room temperature (22°C).

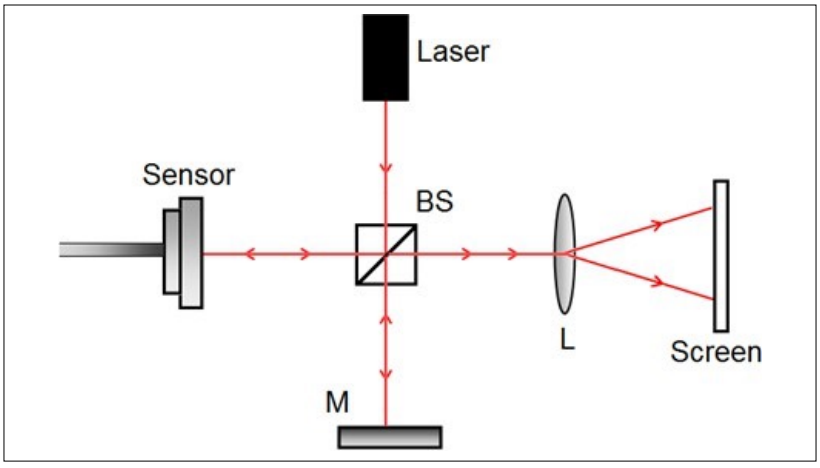

Figure 4: Schematic setup for Michelson interferometry optical measurements.
Source: Elaborated by the authors.

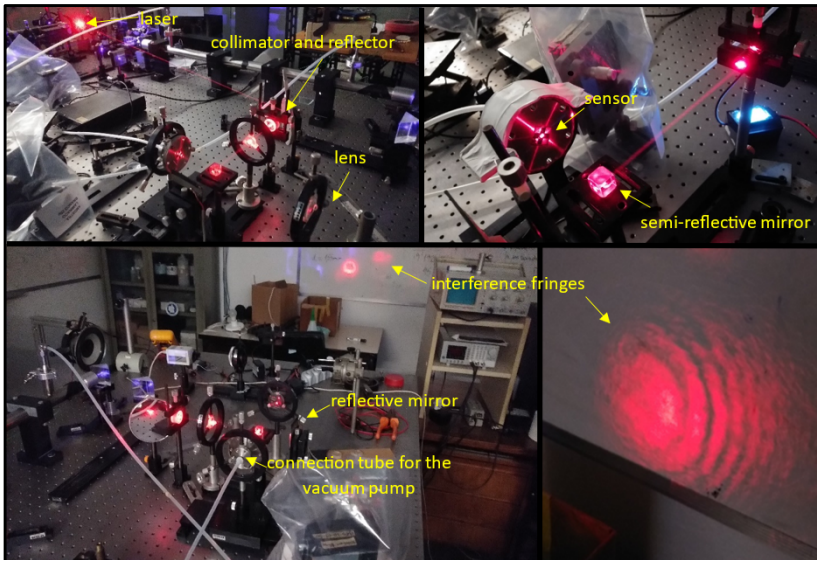

Figure 5: Detailed of the experimental setup for Michelson interferometry optical measurements.
Source: Elaborated by the authors.

RESULTS AND DISCUSSION

Several experiments were performed associating the variation in sensor membrane displacement (y), measured optically in its central region, with the measured pressure (P). Two lasers were used, with wavelengths of 655 nm

and 632.8 nm. The measurements were performed in pumping cycles, described as "Vacuum," and cycles of return to atmospheric pressure, described as "ATM" (Table 1).

Table 1: Interferometry results of the sensor membrane deflection with pressure, for laser at λ = 655 nm.

Vacuum						ATM					
P (mbar)	# Fringes	y (μm)	ΔP (mbar)	ΔP (mbar)	y (μm)	P (mbar)	# Fringes	y (μm)	ΔP (mbar)	ΔP (mbar)	y (μm)
934	0	0,000	912	0	0,000	924	0	0,000	898	0	0,000
808	1	0,328	786	114	0,328	874	1	0,328	848	134	0,328
708	2	0,655	686	219	0,655	806	2	0,655	780	282	0,655
620	3	0,983	598	318	0,983	722	3	0,983	696	392	0,983
530	4	1,310	508	426	1,310	629	4	1,310	603	496	1,310
448	5	1,638	426	508	1,638	522	5	1,638	496	603	1,638
340	6	1,965	318	598	1,965	418	6	1,965	392	696	1,965
241	7	2,293	219	686	2,293	308	7	2,293	282	780	2,293
136	8	2,620	114	786	2,620	160	8	2,620	134	848	2,620
22	9	2,948	0	912	2,948	26	9	2,948	0	898	2,948

Source: Elaborated by the authors.

Considering that the measurement was performed on the upper face of the sensor and pumping occurs on the rear face, the displacement increases with the reduction in measured pressure (Fig. 6). To compare the simulated and theoretical results, the graphs were normalized by the variation in pressure and observed displacements, causing the maximum displacement to occur at maximum pressure. A linear variation of the membrane displacement with pressure is noted, more pronounced during pumping. A possible explanation stems from the different speeds of pressure variation when opening to the atmosphere, which can generate mechanical hysteresis in the membrane.

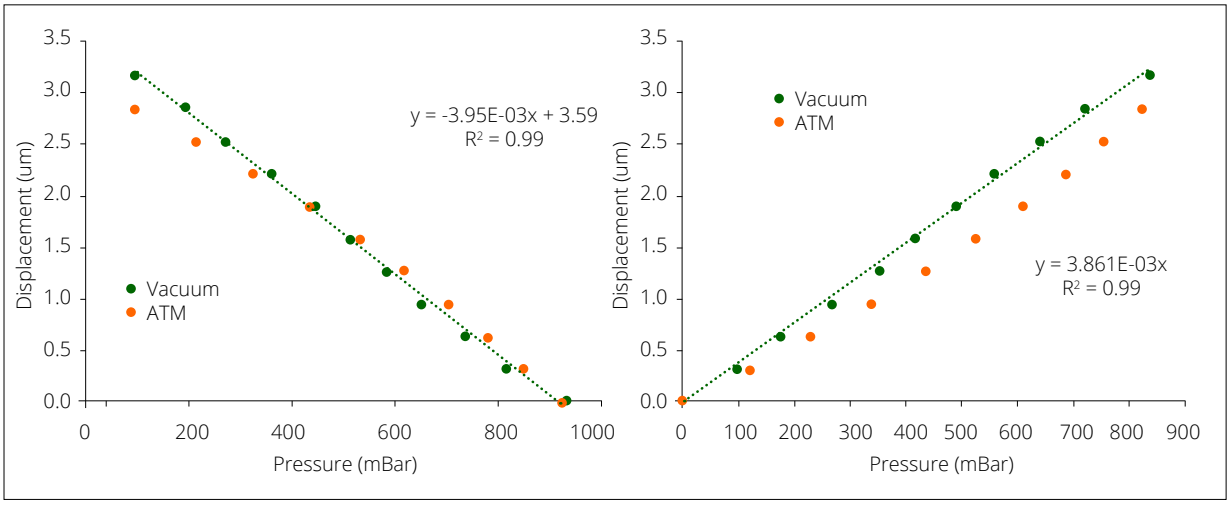

Figure 6: Membrane displacement as a function of pressure for λ = 655 nm. Original measurement (left) and normalized measurement (right). Source: Elaborated by the authors.

Similar behavior was observed when using a light source with λ = 632.8 nm (Table 2 and Fig. 7). In both cases, the linearity presented R2 values very close to unity. Another observation refers to the maximum deflection obtained,

which was 2.948 μm for λ = 655 nm and 3.164 μm for λ = 632.8 nm. Therefore, for a pressure difference of 900 mbar, the measured displacement of the membrane was approximately 3 μm.

Table 2: Interferometry results of the sensor membrane deflection with pressure, for a laser with λ = 632.8 nm.

Vacuum						ATM					
P (mbar)	# Fringes	y (μm)	ΔP (mbar)	ΔP (mbar)	y (μm)	P (mbar)	# Fringes	y (μm)	ΔP (mbar)	ΔP (mbar)	y (μm)
931	0	0,000	836	0	0,000	920	0	0,000	825	0	0,000
816	1	0,316	721	97	0,316	847	1	0,316	752	119	0,316
735	2	0,633	640	175	0,633	780	2	0,633	685	229	0,633
650	3	0,949	555	266	0,949	703	3	0,949	608	339	0,949
584	4	1,266	489	351	1,266	618	4	1,266	523	434	1,266
512	5	1,582	417	417	1,582	529	5	1,582	434	523	1,582
446	6	1,898	351	489	1,898	434	6	1,898	339	608	1,898
361	7	2,215	266	555	2,215	324	7	2,215	229	685	2,215
270	8	2,531	175	640	2,531	214	8	2,531	119	752	2,531
192	9	2,848	97	721	2,848	95	9	2,848	0	825	2,848
95	*10*	*3,164*	*0*	*836*	*3,164*						

Source: Elaborated by the authors.

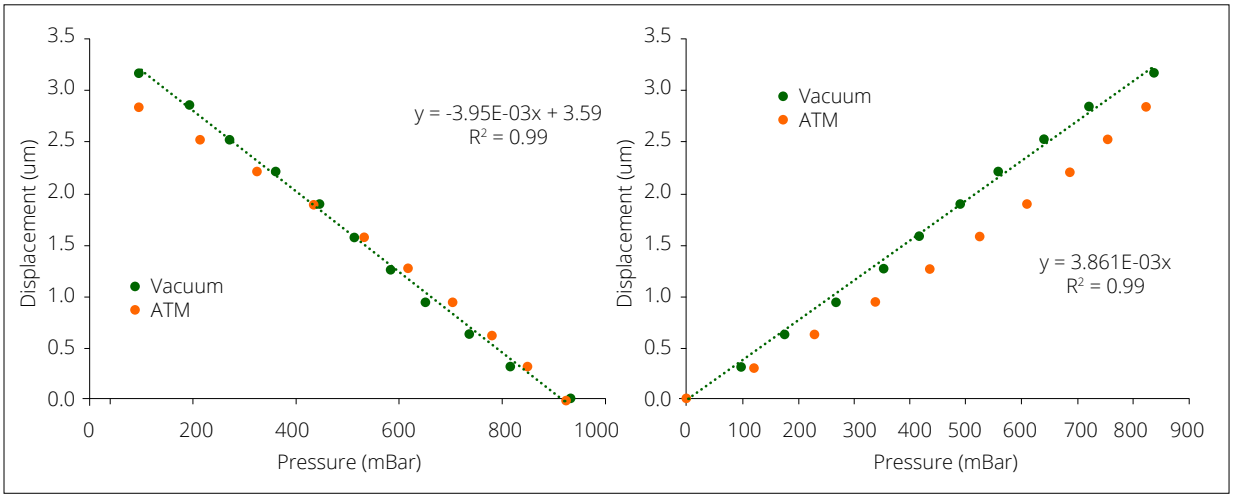

Figure 7: Membrane displacement as a function of pressure for λ = 632.8 nm. Original measurement (left) and normalized measurement (right). Source: Elaborated by the authors.

Using the program COMSOL Multiphysics, it was possible to determine the membrane deflection as a function of applied pressure (Fig. 8). The red line indicates the position used to evaluated the deflection for different membrane thicknesses (Fig. 9).

Analyzing the maximum deflection values for a variation of 900 mbar as a function of membrane thickness, a behavior close to x^{-3} was observed (Fig. 10). For a deflection obtained experimentally in interferometry measurements of 3 μm, the membrane thickness would correspond to 126 μm.

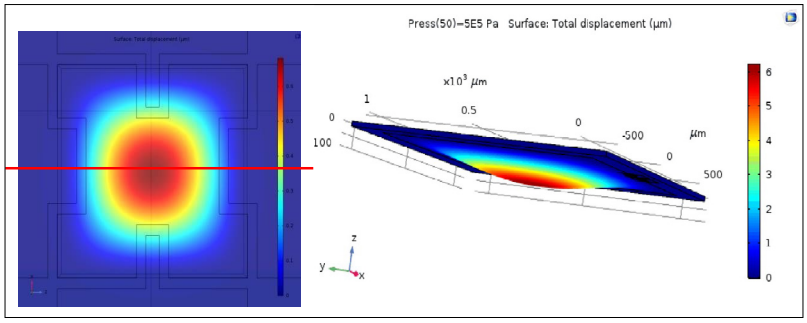

Figure 8: COMSOL Multiphysics simulation of the deflection in the central region of the pressure sensor membrane.

Source: Elaborated by the authors.

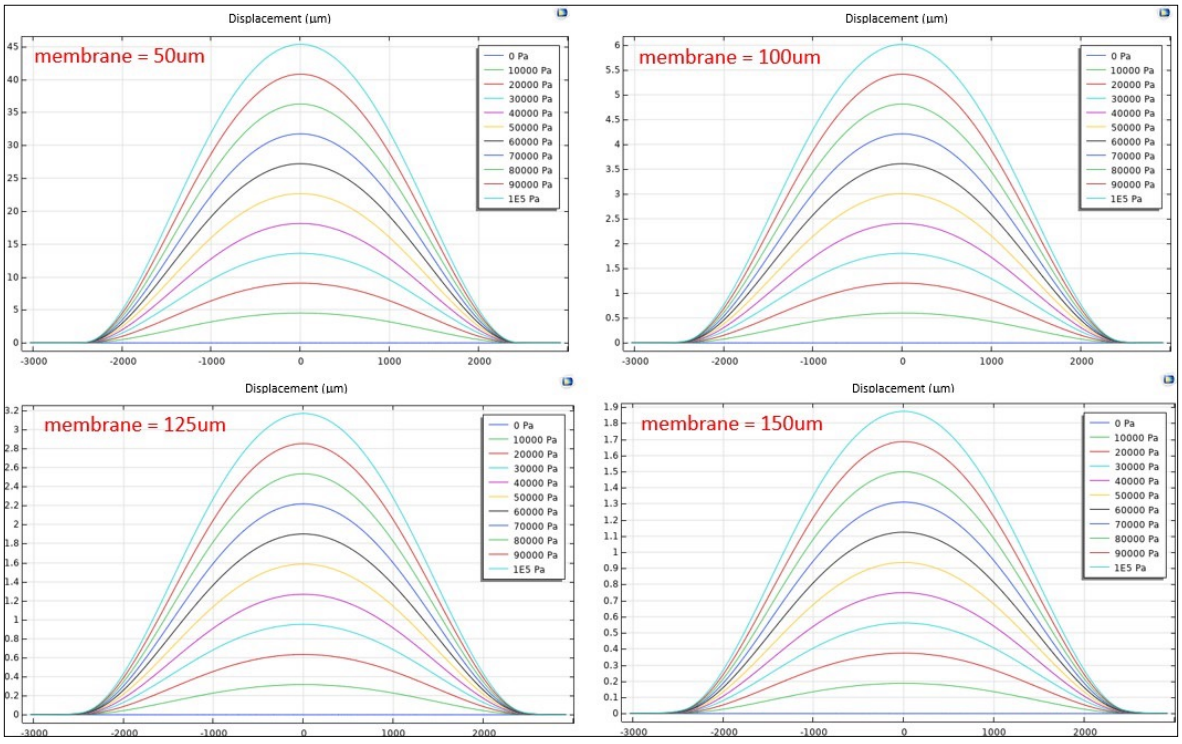

Figure 9: COMSOL Multiphysics simulation of deflection in the central region of the sensor membrane for different applied pressures and different membrane thicknesses. Source: Elaborated by the authors.

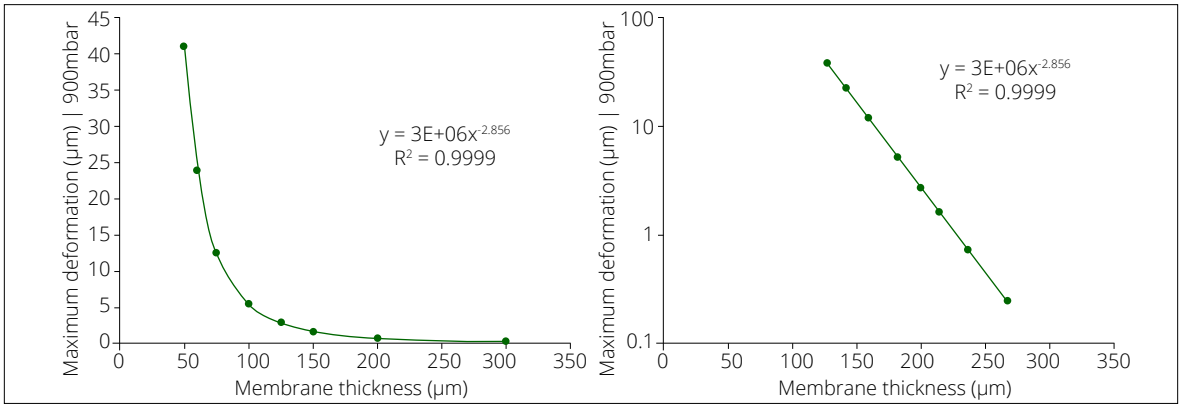

Figure 10: Analysis of the maximum deflection in the central region of the sensor membrane for an applied pressure of 900 mbar as a function of membrane thickness, on a linear (left) and logarithmic (right) scale. Source: Elaborated by the authors.

Considering that fixing the sensor with silicone grease does not constitute a rigid assembly, it is therefore in an intermediate situation between fully engraved and only supported, the condition of convergence between the theoretical, experimental, and simulated values, was explored.

Through the theoretical analysis of clamped plates[10,11], one can relates the maximum deflection (ymax) as a function of the applied pressure (q), plate thickness (t), and square plate width (b) (Eq. 2). It can be noted that the maximum deflection depends linearly on the pressure and inversely on the cube of the plate thickness.

$$y_{max} = \frac{\alpha q b^4}{Et^3} \tag{2}$$

where: E: modulus of elasticity of silicon (E = 1.8.10^{11}N/m^2); α: a constant indicated in Table 3.

Table 3: Theoretical information on the deflection of embedded plates.

Case, shape and supports	Case, loading	Formulas and tabulated specific values							
Rectangular plate, all edges fixed 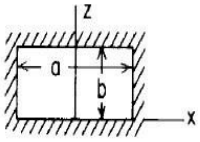	Uniform over entire plate	(At center of long edge) $\sigma_{max} = \frac{-\beta_1 q b^2}{t^2}$							
		(At center) $\sigma = \frac{\beta_2 q b^2}{t^2}$ and $y_{max} = \frac{\alpha q b^4}{Et^3}$							
		a/b	1.0	1.2	1.4	1.6	1.8	2.0	∞
		β_1	0.3078	0.3834	0.4356	0.4680	0.4872	0.4974	0.5000
		β_2	0.1386	0.1794	0.2094	0.2286	0.2406	0.2472	0.2500
		α	0.0138	0.0188	0.0226	0.0251	0.0267	0.0277	0.0284

Source: Young et al.[11].

The determination of the plate width is related to the manufacturing process through anisotropic corrosion of silicon, which reduces the width of the membrane (Wb) from that defined by the corrosion protection mask design (W0), depending on the depth of the corrosion performed[1] (Fig. 11)[12]. Considering that W0 = 5 mm, silicon wafer thickness (t + l) = 415 μm, and membrane thickness t = 126 μm, we obtained Wb = 4.59 μm. Using the theoretical expression, we can obtain the results shown in Fig. 12.

When comparing the theoretical results and simulated with the experimental results of 3 μm for maximum deflection (at 900 mbar), now as a function of membrane thickness, there is no coincidence of values, that is, to obtain 3 μm experimental, the theory indicates a membrane thickness of 103 μm and the simulation 128 μm. By adjusting the membrane width Wb to 5.4 μm, the curves converge to the expected thickness value of t = 126 μm (Fig. 13).

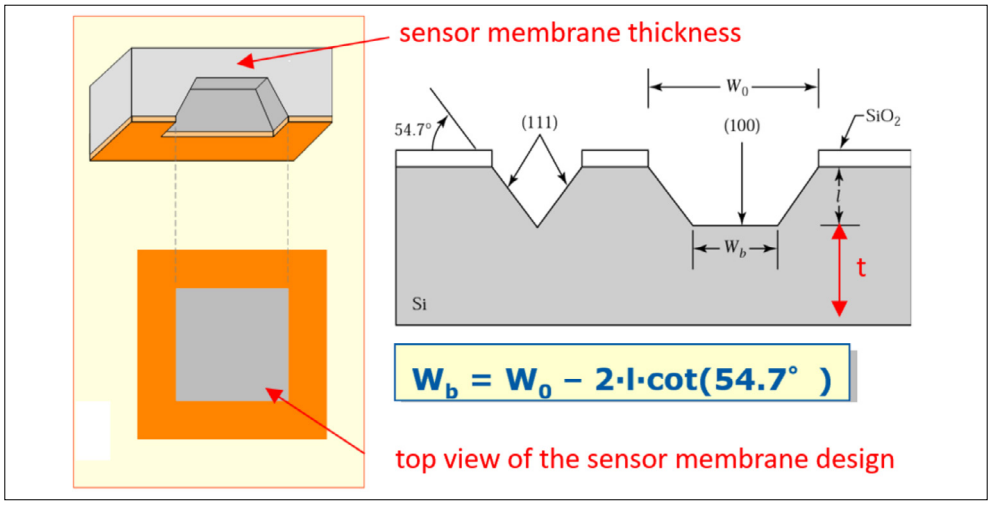

Figure 11: Anisotropic corrosion of silicon to produce the sensor membrane.
Source: Ohlckers and Lapadatu[12].

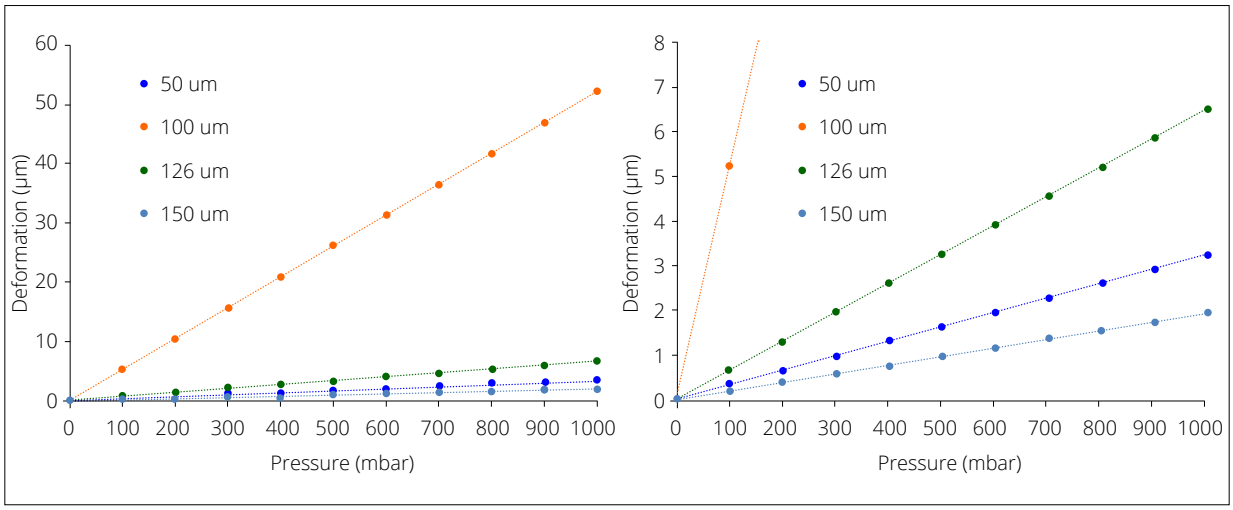

Figure 12: Theoretical analysis of the maximum deflection in the central region of the sensor membrane for different applied pressures and different membrane thicknesses, enlarged on the right. Source: Elaborated by the authors.

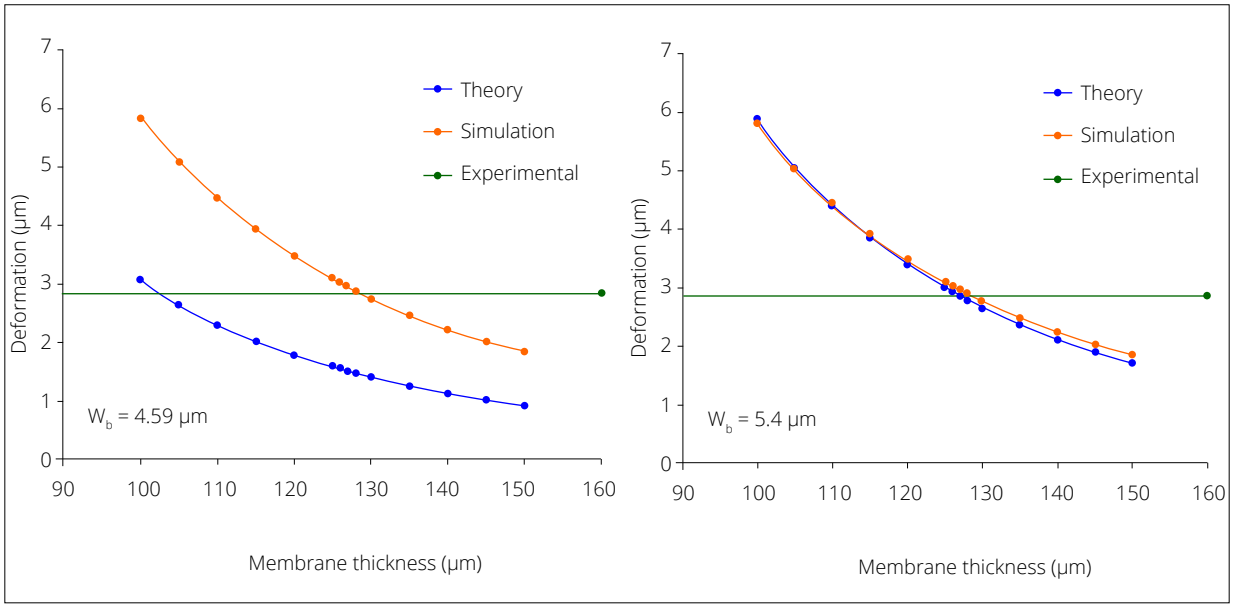

Figure 13: Comparison between theoretical, simulated, and experimental values for maximum deflection for two membrane width values. Source: Elaborated by the authors.

Considering that the design value for W0 = 5 mm was obtained experimentally, the value of Wb must be less than 5 mm. Thus, several comparisons were made of the results obtained from the deflection of the membrane as a function of pressure, changing the factor of membrane thickness, which also affects the Wb factor due to corrosion. The other factors were kept constant.

For a membrane thickness t = 97 µm, there is a coincidence between the theoretical values and the average of all experimental values, but the simulated results are overestimated (Fig. 14), on the other hand, for a membrane thickness t = 122 µm, there is a coincidence between the simulated values and the average of all experimental values, but the theoretical results are underestimated (Fig. 15), finally for a membrane thickness t = 126 µm, none of the values coincide (Fig. 16).

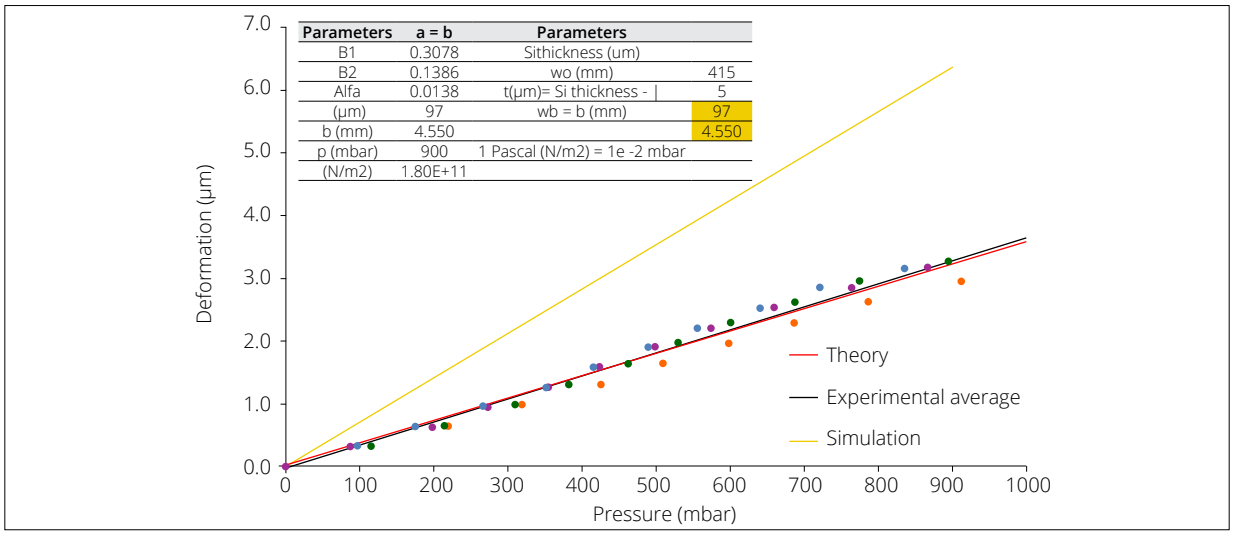

Figure 14: Comparisons of theoretical, experimental, and simulated results obtained from membrane deflection as a function of pressure, t = 97 µm. Source: Elaborated by the authors.

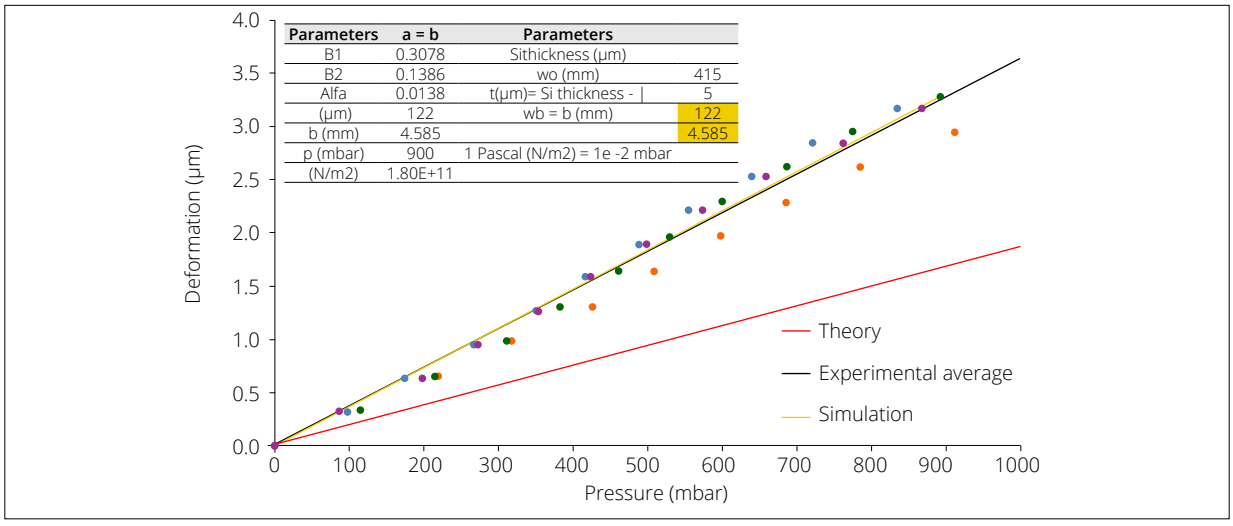

Figure 15: Comparisons of theoretical, experimental, and simulated results obtained from membrane deflection as a function of pressure, for t = 122 µm. Source: Elaborated by the authors.

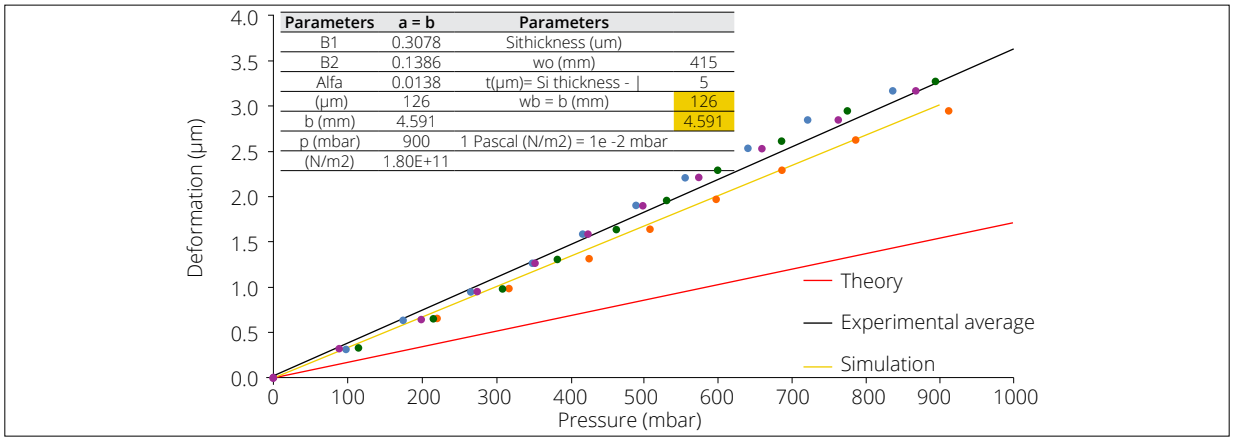

Figure 16: Comparisons of theoretical, experimental, and simulated results obtained from membrane deflection as a function of pressure for t = 126 µm. Source: Elaborated by the authors.

For the situation in which the plate is only supported, the theoretical parameters change, mainly the proportionality factor (α) in Eq. 2, as indicated in Table 4. The maximum deformation equation remains the same.

Table 4: Theoretical information on the deflection of supported plates.

Case, shape and supports	Case, loading	Formulas and tabulated specific values					
Rectangular plate, all edges fixed 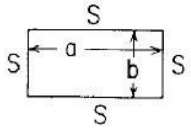	Uniform over entire plate	(At center) $\sigma_{max} = \sigma_b = \frac{\beta q b^2}{t^2}$ and $y_{max} = \frac{-\alpha q b^4}{Et^3}$					
		(At center of long sides) $R_{max} = \gamma q b$					
		a/b	1.0	1.2	1.4	1.6	1.8
		β	0.2874	0.3762	0.4530	0.5172	0.5688
		α	0.0444	0.0616	0.0770	0.0903	0.1017
		γ	0.420	0.455	0.478	0.491	0.499

Source: Young et al.[11].

The value that enabled convergence was α = 0.027 (Fig. 17). Considering the values of the fully fixed plate (α = 0.0138) and the fully free plate (α = 0.0444), and calculating the average, we have α = 0.0291, indicating that the sensor would be close to the average value.

Thus, the convergence condition between all situations analyzed for the pressure sensor is shown in Table 5.

Table 5: Convergence values for experimental, simulated, and theoretical measurements

Parameters	a = b	Parameters	
B1	0.3078	Si thickness (μm)	415
B2	0.1386	w0 (mm)	5
Alfa	0.027	t (μm) = Si thickness - l	122
t(μm)	122	wb = b (mm)	4.585
b(mm)	4.585		
p (mbar)	900	1 Pascal (N/m2) = 1e-2 mbar	
E(N/m2)	1.80E + 11		

Source: Elaborated by the authors.

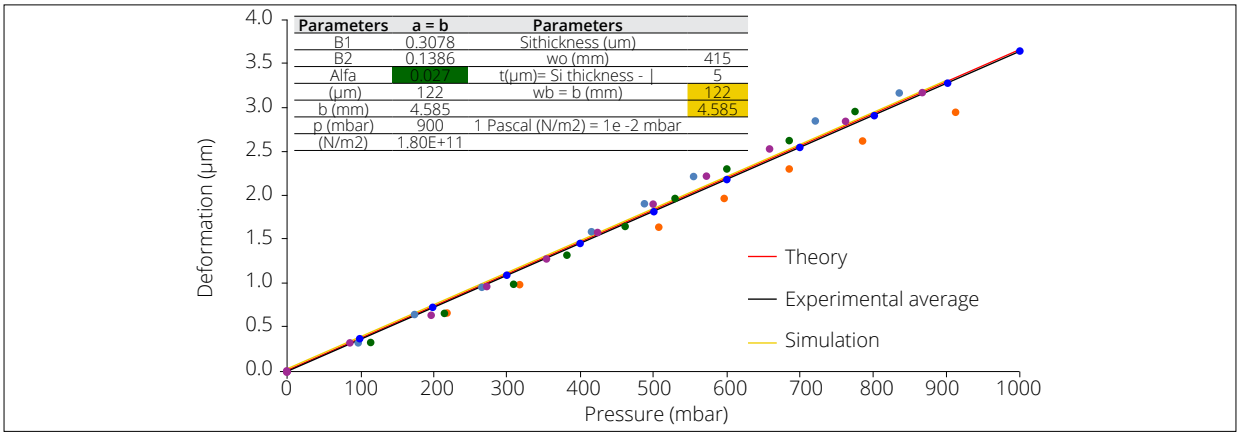

Figure 17: Comparisons of theoretical, experimental, and simulated results obtained from membrane deflection as a function of pressure, for t = 122 μm and α = 0.027. Source: Elaborated by the authors.

CONCLUSION

This study proposed the direct determination of membrane deflection as a function of applied pressure through optical measurements using Michelson interferometry in a pressure microsensor manufactured using MEMS technology. The pressure microsensor is based on piezoresistors diffused on a silicon membrane, obtained by the process of anisotropic corrosion of silicon in potassium hydroxide, whose measurement pattern is the electrical response obtained through a Wheatstone bridge circuit, in which the potential difference (Vout) is a function of the resistance variation of the piezoresistors subjected to pressure.

The results obtained with the aid of the Michelson interferometer, using lasers with wavelengths of λ = 655 and 632.8 nm, showed linear membrane deflection with pressure in the region of 900 mbar. Hysteresis was observed in the measurements, which may be associated with the different rates of pressure variation applied. The maximum deflection observed was 3 µm. Considering all the optical results, a variation of 3.61 µm/bar was obtained.

Analyses using the COMSOL Multiphysics simulator indicated that the maximum deflection of the membrane is approximately inversely proportional to the cube (2.85) of the membrane thickness, consistent with what is suggested theoretically.

The comparative results of the experimental measurements with the simulated and theoretical ones indicated that the membrane has a thickness of 122 µm and 4.58 mm on each side and suggest that the sensor's clamping is close to the average between free clamping and fully clamped.

Pressure is the most measured physical quantity in industrial, scientific, and technological activities. The results presented suggest that the low-cost pressure microsensor developed can be evaluated simultaneously by electrical and optical measurements, expanding its usefulness and application, enabling pressure measurement based on the mechanical definition of pressure and not depending on the type of gas. Future work is being considered to optimize the sensitivity of the sensor by varying the area and thickness of the silicon membrane, as well as manufacturing using additive manufacturing technologies.

CONFLICT OF INTEREST

Nothing to declare.

AUTHOR CONTRIBUTIONS

Conceptualization: Fontes MBA, Barbosa EA, Pauletti RMO, Degasperi FT; **Formal Analysis:** Fontes MBA, Barbosa EA, Pauletti RMO, Degasperi FT; **Investigation:** Fontes MBA, Barbosa EA, Pauletti RMO, Degasperi FT; **Resources:** Fontes MBA, Barbosa EA, Pauletti RMO, Degasperi FT; **Supervision:** Degasperi FT; **Validation:** Fontes MBA, Barbosa EA, Pauletti RMO, Degasperi FT; **Data curation:** Fontes MBA, Barbosa EA, Pauletti RMO, Degasperi FT; **Writing – review and editing:** Fontes MBA, Barbosa EA, Pauletti RMO, Degasperi FT; **Final approval:** Fontes MBA.

AVAILABILITY OF DATA AND MATERIALS

All dataset were generated or analyzed in the current study.

FUNDING

Not applicable.

DECLARATION OF USE OF ARTIFICIAL INTELLIGENCE TOOLS

The authors declare that no artificial intelligence tools were used in the preparation, writing, data analysis, or review of this manuscript.

ACKNOWLEDGEMENTS

To the infrastructure of the Applied Optics Laboratory and Vacuum Technology Laboratory of the Faculdade de Tecnologia de São Paulo.

REFERENCES

1. Madou M. Fundamentals of microfabrication and nanotechnology. 3. ed. Boca Raton: CRC Press; 2011. 3 v. https://doi.org/10.1201/9781315274164
2. Maluf N. An introduction to microelectromechanical systems engineering. Meas Sci Technol. 2002;13(2):229.
3. Coraucci GO. Sensor de Pressão Microeletrônico Baseado no Efeito Piezoresistivo Transversal em Silício" Tese de doutorado, Faculdade de Engenharia Elétrica e Computação da Universidade Estadual de Campinas, 2008. https://doi.org/10.47749/T/UNICAMP.2008.437621
4. Benedict RP. Fundamentals of temperature, pressure, and flow measurements. 3. ed. New York: John Wiley; 1984.
5. Sanches KF, Tabiku HDS, Zambom LS, Fontes MBA. Desenvolvimento de um Microssensor de Pressão Microeletromecânico. Boletim Técnico da Faculdade de Tecnologia de São Paulo, BT47, p. 17-22, 2019. https://bt.fatecsp.br/bulletins/show_article/1072
6. Wikipédia. Interferometria. Wikipédia; 2022 [cited Aug 21, 2024]. Available at: https://pt.wikipedia.org/wiki/Interferometria
7. Carvalho PRB. Construção e Caracterização de um Atuador Piezocerâmico, Trabalho de Conclusão de Curso (TCC). https://biblioteca.fatecsp.br/shared/biblio_view.php?bibid=18727&tab=opac
8. Santos JBS, Helfstein HA, Saita MT, Degasperi FT, Torres RB, Barbosa EA. Gas mixture analysis by temperature-independent, multi-wavelength refractive mixing rules. J Chem Thermodyn. 2025; 206: 107473. https://doi.org/10.1016/j.jct.2025.107473
9. COMSOL. Portal [cited Apr 5, 2024]. Available at: https://www.comsol.com
10. Fraga MA, Koberstein LL, Rasia LA, Charry E. Método analítico para dimensionamento do diafragma de um sensor de pressão piezoresistivo. In: XI IBERCHIP; 2004; Cartagena de Índias, Colômbia. https://www.academia.edu/download/65830507/MTODO_ANALTICO_PARA_DIMENSIONAMENTO_DO_D20210228-31722-1hx9g9n.pdf
11. Young WC, Budynas RG, Sadegh AM. Roark's formulas for stress and strain. New York: McGraw-Hill Education; 2012. https://www.academia.edu/download/54667870/Roarks_formulas_for_stress_and_strain.pdf
12. Ohlckers P, Lapadatu D. Wet bulk micromachining. Slide Serve; 2011 [cited Feb 15, 2024]. Available at: https://www.slideserve.com/anneke/wet-bulk-micromachining